ARTICLE

ACS chemical biology

In Vivo Structure–Activity Relationship Study of Dorsomorphin Analogues Identifies Selective VEGF and BMP Inhibitors

Jijun Hao[†], Joshua N. Ho[†], Jana A. Lewis[‡], Kaleh A. Karim[†], R. Nathan Daniels[§], Patrick R. Gentry[‡,∥], Corey R. Hopkins[‡,∥], Craig W. Lindsley[‡,§,∥,⊥], and Charles C. Hong[†,‡,⊥,#,*]

[†]Division of Cardiovascular Medicine, Department of Medicine, [‡]Department of Pharmacology, [§]Department of Chemistry, [∥]Vanderbilt Program in Drug Discovery, [⊥]Vanderbilt Institute of Chemical Biology, Vanderbilt University School of Medicine, Nashville, Tennessee 37232, and [#]Research Medicine, Veterans Administration TVHS, Nashville, Tennessee 37212

ABSTRACT The therapeutic potential of small molecule signaling inhibitors is often limited by off-target effects. Recently, in a screen for compounds that perturb the zebrafish embryonic dorsoventral axis, we identified dorsomorphin, the first selective inhibitor of bone morphogenetic protein (BMP) signaling. Here we show that dorsomorphin has significant "off-target" effects against the VEGF (vascular endothelial growth factor) type-2 receptor (Flk1/KDR) and disrupts zebrafish angiogenesis. Since both BMP and VEGF signals are known to be involved in vascular development, we sought to determine whether dorsomorphin's antiangiogenic effects are due to its impact on the BMP or VEGF signals through the development of analogues that target BMP but not VEGF signaling and *vice versa*. In a structure–activity relationship (SAR) study of dorsomorphin analogues based primarily on their effects on live zebrafish embryos, we identified highly selective and potent BMP inhibitors as well as selective VEGF inhibitors. One of the BMP inhibitors, DMH1, which exclusively targets the BMP but not the VEGF pathway, dorsalized the embryonic axis without disrupting the angiogenic process, demonstrating that BMP signaling was not involved in the angiogenic process. This is one of the first full-scale SAR studies performed in vertebrates and demonstrates the potential of zebrafish as an attractive complementary platform for drug development that incorporates an assessment of *in vivo* bioactivity and selectivity in the context of a living organism.

With advances in high-throughput screening capabilities, it is not difficult to identify compounds that target a particular protein or pathway. Rather, a greater challenge lies in identifying selective modulators and improving pharmaceutical, or ADMET (absorption, distribution, metabolism, excretion, and toxicity), properties of lead compounds (*1*). In the traditional approach to pharmaceutical development, the initial efforts at lead optimization are focused on identifying structural analogues with the highest potency against a therapeutic target in *in vitro* assays. However, when the subsequent *in vivo* results clash with the predictions based on *in vitro* tests, it is difficult to determine whether such "failures" result from flawed biological underpinnings or compounds' intrinsic deficiencies, such as poor target selectivity or suboptimal *in vivo* bioavailability.

In principal, these pitfalls can be circumvented with the use of the *in vivo* zebrafish model early in the lead optimization phase. Rapid external development, transparency, and high fecundity make zebrafish ideal for large-scale *in vivo* characterization of bioactive small molecules (*2*–*5*). Since embryonic cells are capable of integrating multiple signaling pathways to trigger precise developmental outputs, a small molecule that selectively targets a signaling pathway involved in embryonic patterning will phenocopy genetic mutations in that pathway, whereas nonspecific compounds will cause early embryonic lethality or nonspecific developmental delay. In addition, since drug exposure in embryos occurs by passive diffusion, the *in vivo* assessment takes into account compounds' intrinsic physiochemical prop-

*Corresponding author, charles.c.hong@vanderbilt.edu.

Received for review November 12, 2009 and accepted December 19, 2009.

Published online December 20, 2009

10.1021/cb9002865

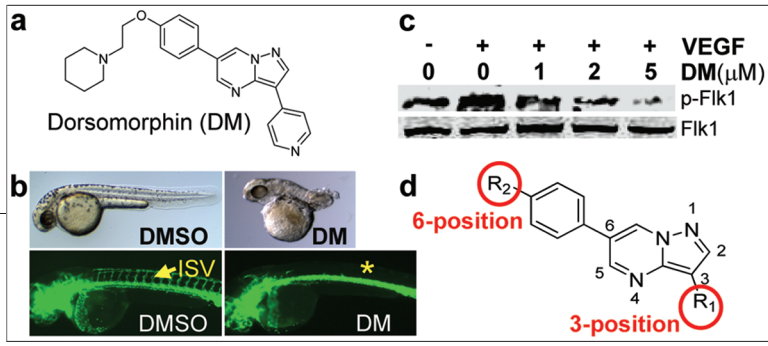

Figure 1. Inhibition of both BMP and VEGF signaling by dorsomorphin, and the pyrazolo[1,5-*a*]pyrimidine backbone of DM for derivatization. a) Structure of dorsomorphin (DM). b) DM at a concentration of 2 μM dorsalized zebrafish embryos when administered at 3 h post fertilization (hpf), and 10 μM DM blocked intersomitic vessel (ISV) formation when administered at 12 hpf. Above, bright-field images of treated embryos. Below, green fluorescence images of the *Tg(Fli:EGFP)y1* transgenic embryos, which express GFP in the vasculature. Control embryos treated with DMSO are on the left, and DM-treated embryos are on the right. c) DM suppressed VEGF-dependent Flk1 phosphorylation in a dose-dependent manner in bovine arterial endothelial cells (BAECs). d) The pyrazolo[1,5-*a*]pyrimidine backbone of DM for derivatization involving modifications at the 3- and 6-positions (red circles).

erties, such as the octanol−water partition coefficient (commonly referred to as log *P*), a major determinant of drug-likeness and bioactivity of a small molecule (*6*). As a proof-of-principle, we identified dorsomorphin (Figure 1, panel a), the first selective small molecule inhibitor of BMP signaling, on the basis of its ability to phenocopy the dorsoventral (DV) pattern defects seen in the BMP pathway mutants (Figure 1, panel b) (*7*).

Dorsomorphin and its analogue LDN-193189 have been used to direct differentiation of stem cells and to demonstrate the therapeutic potential of targeting BMP signals for anemia and hyperossification syndromes (*7–9*). In particular, the discovery of dorsomorphin has immediate therapeutic implications for a debilitating heretofore incurable condition known as fibrodysplasia ossificans progressiva, which has recently been shown to be caused by activating mutations in ALK2 (ACVR1), a BMP type-I receptor (*10–12*).

However, enthusiasm regarding their utility and therapeutic potential is tempered by the fact that dorsomorphin had significant "off-target" effects, including AMPK inhibition (*13*). Since AMPK plays a central role in energy metabolism and is known to have beneficial cardiovascular and antitumor effects, inhibiting AMPK has potential to cause cardiotoxicity and promote tumorigenesis (*14–16*). Here we show that dorsomorphin also had significant inhibitory activity against the VEGF signaling and caused a significant defect in the intersomitic vessel (ISV) formation, an angiogenic process known to require signaling by the VEGF type-II receptor (also known as Vegfr2/Kdr/Flk1) (*17–20*). However, because BMP signaling is also known to be involved in angiogenesis (*21, 22*), it was possible that dorsomorphin treatment revealed a novel role of the BMP signal in ISV formation.

To distinguish between these possibilities and to generate additional potent and specific BMP and VEGF inhibitors, we undertook a large-scale *in vivo* SAR study of dorsomorphin analogues based on their effects on zebrafish embryos. We synthesized 63 distinct compounds using the parallel library synthesis approach and tested them in zebrafish embryos to identify highly selective and potent inhibitors of BMP as well as VEGF signaling. One of the analogues, DMH1, which exclusively targets BMP but not VEGF signaling, dorsalized the embryonic axis without disrupting ISV formation, demonstrating that BMP signaling is not required for zebrafish ISV formation.

RESULTS AND DISCUSSION

During the course of characterizing the effects of dorsomorphin (Figure 1, panel a) in zebrafish embryos, we found that it consistently caused significant defects in ISV formation (Figure 1, panel b), an angiogenic process known to require signaling by the VEGF type-II receptors (Kdr/Flk1) (*23*). To examine in detail dorsomorphin's effects on ISV formation, the *Tg(fli:1a:EGFP)y1* transgenic embryos expressing GFP under the control of an endothelial-specific promoter (*24*) were treated with various concentrations (0.1−100 μM) of dorsomorphin starting at 12 h post fertilization (hpf). Because this stage follows the establishment of the dorsoventral (DV) axis, this analysis focused only on dorsomorphin's effects on angiogenesis. After dorsomorphin treatment, ISV was visualized in live 48 hpf embryos. In this *in vivo* angiogenesis model, dorsomorphin completely inhibited ISV formation at 10 μM (Figure 1, panel b). At 5 μM, roughly 50% of the ISV were severely shortened or eliminated (dorsomorphin's EC50, effective concentration affecting 50% of ISVs, was therefore 5 μM; Table 1).

In cultured bovine aortic endothelial cells, dorsomorphin inhibited the VEGF-stimulated Flk1 phosphorylation in a dose-dependent manner (Figure 1, panel c), demonstrating that dorsomorphin was a potent VEGF signal inhibitor. Nevertheless, since BMP signaling is also known to be involved in angiogenesis (*21, 22*), it was formally possible that dorsomorphin's effects on the zebrafish vasculature revealed a novel role of the BMP signal in ISV formation. To test this, we sought to develop small molecules that specifically inhibited BMP but not VEGF signaling.

TABLE 1. *In vivo* assessments and *in vitro* kinase assays of DM and selected analogues[a]

Compound	R1	R2	Dorsalization (EC100, μM)	ISV disruption (EC50, μM)	Toxicity (EC100, μM)
DM		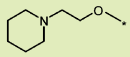	2.5	5	20
LDN-193189			3	20	20
6LE		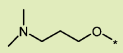	5	50	No (>50)
6K1		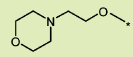	1	5	20
91E			2	2	5
6LP			No (>50)	No (>50)	No (>50)
DMH1			0.2	No (>50)	No (>50)
DMH2		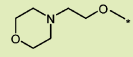	0.1	No (>50)	25
DMH3		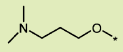	1	No (>50)	No (>50)
DMH4		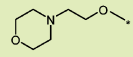	No (>50)	1	No (>50)
SU5146	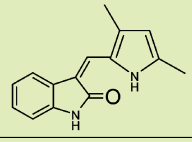		No	2	5

[a]Dorsomorphin (DM) and the selected analogues, along with the R1 and R2 structural modifications and the effects on zebrafish embryos with respect to the dorsoventral (DV) axis, the intersomitic vessel (ISV) disruption, and nonspecific toxicity. For dorsalization, the EC100 (effective concentration 100%) represents the concentration when 100% of the treated embryos are severely dorsalized. As a result of significant day-to-day variability in severity of dorsalization at "sub-threshold" concentrations, the EC50 for severe dorsalization could not be reliably determined. For ISV disruption, the EC50 represents the concentration when the formation of about 50% of the ISVs is inhibited. For nonspecific toxicity, the EC100 represents the concentration when 100% of the treated embryos exhibit either early lethality within hours of compound addition, variable embryonic defects, or developmental delay. For comparison, the effects of the known KDR inhibitor SU5416 are shown at the bottom. Results from at least 20 embryos per condition.

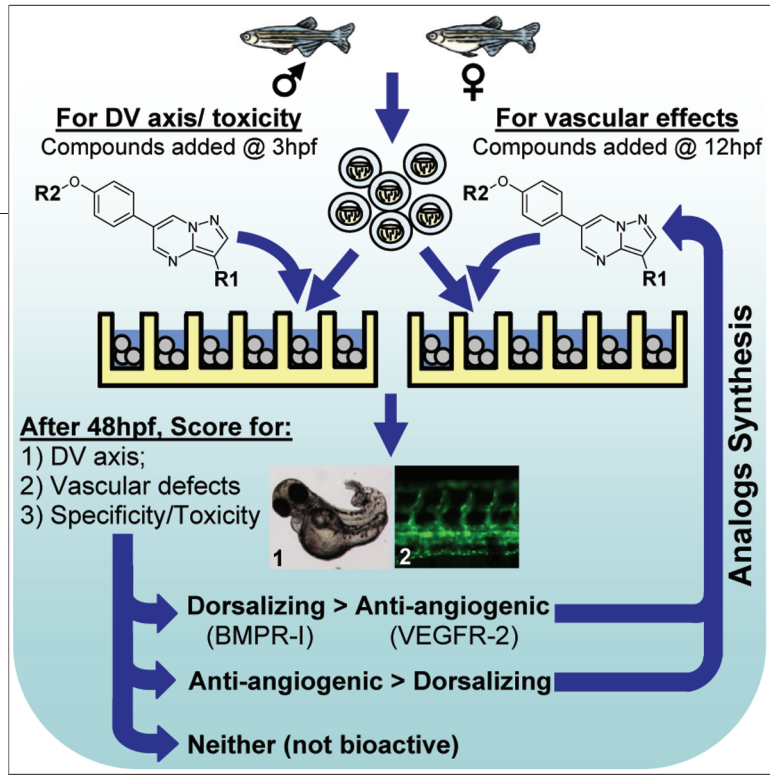

Figure 2. Schema of zebrafish-based structure−activity relationship (SAR) study of DM analogues. To assess each analogue's effect on the dorsoventral (DV) axis, the wild-type embryos were exposed to the compound (at concentration from 0.01 to 50 μM) starting at 3 hpf. To assess each analogue's effect on angiogenesis, the *Tg-(Fli:EGFP)y1* embryos were exposed to each compound (from 0.01 to 50 μM) starting at 12 hpf. After 48 h, the compound-treated embryos were manually scored for dorsalization of the DV axis (BMPR-I inhibition), vascular defects (VEGFR-2 inhibition), and nonspecific toxicity or defects. The compounds that caused dorsalization or blocked angiogenesis were considered for the subsequent round of analogue synthesis and testing.

To generate additional potent and specific BMP inhibitors, we synthesized a number of molecules centered around the 3,6-disubstituted pyrazolo[1,5-*a*]pyrimidine core of dorsomorphin (Figure 1, panel d; Supplementary Figure S1; Supplementary Tables S1, S2). Our effort was concentrated on varying two aspects of the dorsomorphin structure: the R_1 group (C-3 of the core structure) and the R_2 group (4-phenyl group on C-6 of the core structure) (Figure 1, panel d; Supplementary Tables S1, S2) (*25*). The parallel library synthesis, as detailed in Supporting Information, led to the synthesis and isolation of 63 distinct compounds (Supplementary Tables S1, S2).

Rather than the traditional approach of identifying structural analogues with the highest potency against BMP signaling in *in vitro* assays, the lead optimization effort was driven by the compounds' effects on live zebrafish embryos (Figure 2). *In vivo* effective concentrations (ECs) and relative selectivities against BMP signaling were assessed after administering the compounds at 3 hpf. Because this stage represents a key temporal landmark in zebrafish development when multiple cell signaling pathways fashion the initial embryonic pattern, nonselective inhibitors will cause early lethality or nonspecific developmental defects, whereas the effects of selective BMP inhibitors will be limited to dorsalization of the embryonic axis. Of the initial set of 21 dorsomorphin analogues involving the modifications in the 6-position of the pyrazolo[1,5-*a*]pyrimidine backbone, 9 caused dorsalization without any associated early lethality, 7 caused early lethality, and 5 had no visible effect (Supplementary Table S1). Among the 9 dorsalizing compounds, those with the lower effective concentrations (ECs) were deemed to have greater anti-BMP potency *in vivo*. In this *in vivo* selectivity assessment, both dorsomorphin and the previously reported analogue LDN-193189 (*9*) caused substantial early lethality at 20 μM, suggesting significant off-target effects (Table 1).

Next, we examined the effects of the initial set of analogues and LDN-193189 on ISV formation by administering the compounds at 12 hpf and visualizing the ISV in live 48 hpf *Tg(fli:1a:EGFP)y1* embryos. When the compounds were added at this stage, none caused gross morphologic defects or lethality within 24 h of administration. In this analysis of *in vivo* angiogenesis, LDN-193189 significantly inhibited ISV formation at 20 μM (Table 1). Of the initial 21 analogues, 7 had no effect on ISV formation (Table S1). Of these 7, two (92Y and 6L1) affected the DV axis, but only at high concentrations, indicating poor bioactivity (Table S1). The remaining five had no detectable *in vivo* activity, affecting neither ISV formation nor DV axis. Interestingly, included in this "inactive" group was 6LP, which was previously shown to have significant *in vitro* activity against KDR (IC50, concentration causing 50% inhibition, of 37nM) (*26*) (Supplementary Table 1). This discrepancy highlights the key fact that *in vitro* results do not necessarily predict *in vivo* bioactivity, presumably because they do not take into account a compound's solubility or bioavailability. The remaining 14 initial analogues affected both ISV formation and DV axis, although the individual impact on ISV formation and DV axis varied (Supplementary Table S1). In summary, the modifications at the 6-position had only a modest impact on conferring the selectivity for the DV axis. Thus, an additional round of derivatization was performed retaining several of the 6-position modifications (specifically analogues 6LE, 6K1, and 91E) that conferred enhanced bioactivity or relative selectivity and introducing modifications at the 3-position (Table 1; Supplementary Table S2).

The modifications to the 3-position had a major impact on *in vivo* bioactivity and selectivity (Supplementary Table S2). Specifically, replacement of the 4-pyridyl group at the 3-position with a 4-quinoline group (*9, 27*) resulted in compounds with preferentially greater effect on DV axis over ISV formation (Table 1). Of particular interest were DMH1, DMH2, and DMH3, which did not have any detectible effect on ISV formation (Figure 3; Table 1; Figure 4, panel a). The EC100s for dorsalization (effective concentration causing 100% of embryos to be severely dorsalized) were approximately 0.2, 0.1, and 1 μM for DMH1, DMH2, and DMH3, respectively, in comparison to 2 and 3 μM for dorsomorphin and LDN-193189, respectively (Table 1). DMH2 was the most potent dorsalizing compound but less selective than DMH1 and DHM3 since it caused nonspecific developmental effects at higher concentrations (Table 1).

Replacement of the 4-pyridiyl group at the 3-position with a phenyl group resulted in compounds that preferentially effected ISV formation but not the DV axis (Table 1). For example, DMH4, which had no discernible effect on the DV axis, caused significant defects in the ISV and the subintestinal vessel (SIV) (Figure 3; Table 1; Figure 5, panels a and b). Similar vascular defects have been noted in *kdra* mutants or in larvae treated with the Vegfr2 inhibitor SU5146 (*19, 20*). DMH4's EC50 for ISV inhibition (effective concentration causing loss of 50% of ISVs) was 1 μM, compared to 5 μM for dorsomorphin (Table 1).

Next, we examined the effects of DMH1, DMH2, and DMH3, the analogues exhibiting highest selectivity for DV patterning, in a number of *in vitro* assays. In a BMP-responsive luciferase reporter assay (*28*), the IC50s for DMH1, DMH2, and DMH3 were found to be approximately 100, 20, and 7 nM, respectively (Figure 4, panel b; Supplementary Figure S2). In addition, *in vitro* assays using the purified human BMP type-I receptor ALK2 (activin receptor like kinase-2) confirmed that DMH1, DMH2, and DMH3 were direct inhibitors of ALK2 (IC50s of 107.9, 42.8, and 26.7 nM, respectively) (Table 2).

Consistent with their minimal effect on ISV formation, *in vitro* assays using the purified human KDR demonstrated that DMH1, DMH2, and DMH3 had greatly diminished KDR activity in comparison to that of dorsomorphin and LDN-193189 (IC50 of >30, 2.4, and 2 μM versus 25.1 and 214.7 nM, respectively; Table 2). Additional *in vitro* testing with the purified TGFβ recep-

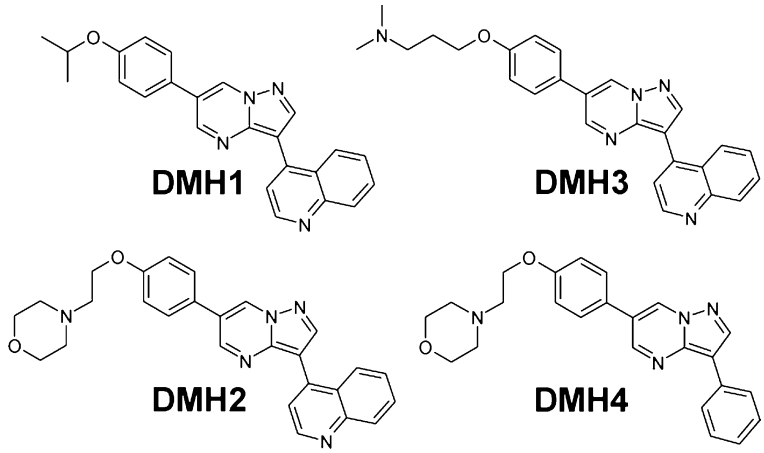

Figure 3. Chemical Structures, IUPAC nomenclature, and LC/MS analyses of DMH1, DMH2, DMH3, and DMH4. DMH1: 4-(6-(4-isopropoxyphenyl)pyrazolo[1,5-*a*]pyrimidin-3-yl)quinoline; >98% at 214 nM, t_R = 2.48 min, *m/z* = 381.2 [M + H]. DMH2: 4-(2-(4-(3-(quinolin-4-yl)pyrazolo[1,5-*a*]pyrimidin-6-yl)phenoxy)ethyl)morpholine; >98% at 214 nM, t_R = 0.72 min, *m/z* = 452.2 [M + H]. DMH3: *N,N*-dimethyl-3-(4-(3-(quinolin-4-yl)pyrazolo[1,5-*a*]pyrimidin-6-yl)phenoxy)propan-1-amine; >98% at 214 nM, t_R = 0.76 min, *m/z* = 424.3 [M + H]. DMH4: 4-(2-(4-(3-phenylpyrazolo[1,5-*a*]pyrimidin-6-yl)phenoxy)ethyl)morpholine; >98% at 214 nM, t_R = 0.89 min, *m/z* = 401.2 [M + H].

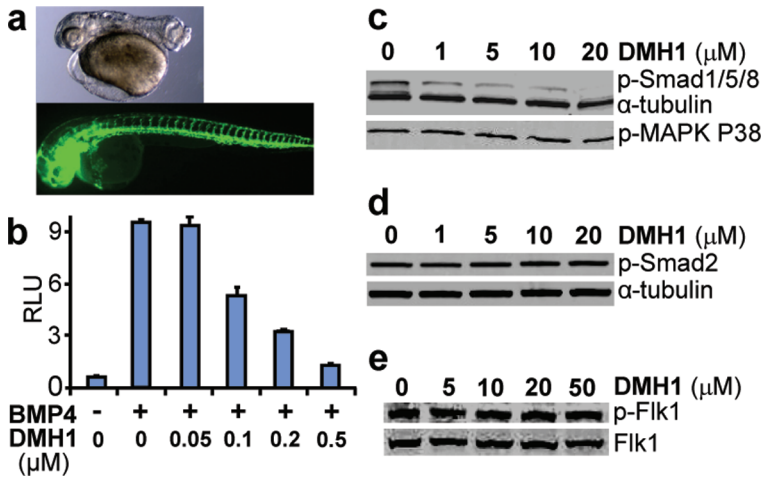

Figure 4. DMH1 is a potent and selective inhibitor of BMP signaling. a) DMH1 (0.2 μM) caused severe dorsalization when the embryos were treated from 3 hpf (above), but it (100 μM) had no effect on ISV formation when the embryos were treated from 12 hpf (below, green fluorescence marks vascular endothelium). b) DMH1 inhibited BMP signaling in a dose-dependent manner in BMP-responsive luciferase reporter assay. RLU (relative luciferase units). c) DMH1 blocked BMP4-induced Smad 1/5/8 phosphorylation in HEK293 cells. In contrast, DMH1 had no effect on (c) BMP4-induced p38 MAPK phosphorylation, and on (d) Activin A-induced Smad2 phosphorylation in HEK293 cells. (e) DMH1 had no effect on VEGF-induced Flk1 phosphorylation in BAECs.

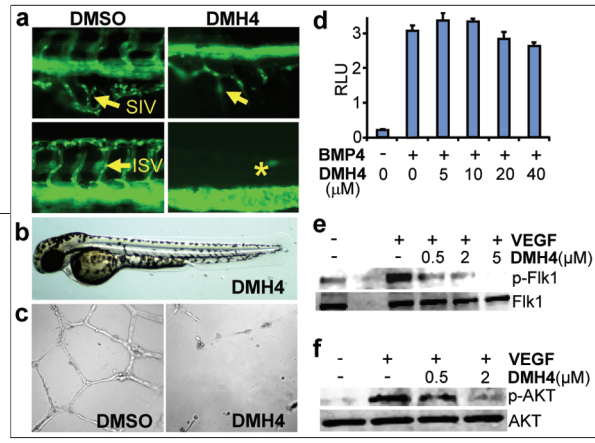

Figure 5. DMH4 is a potent and selective inhibitor of VEGF signaling. a) DMH4 disrupted both ISV and SIV formation at 1 μM. Fluorescent vascular images of DMSO-treated embryo are shown on the left of DMH4-treated embryos. b) DMH4 had no effect on dorsoventral axis at 50 μM when treated from 3 hpf. c) DMH4 (1 μM) blocked VEGF-induced tubular network formation in HUVECs. d) DMH4 did not show significant inhibition of BMP signaling in a BMP-responsive luciferase reporter assay, but it blocked VEGF-induced phosphorylation of Flk1 (e) and (f) AKT in BAECs.

tor ALK5, the AMPK, and the platelet-derived growth factor receptor-β (PDGFRβ) demonstrated that DMH1, DMH2, and DMH3 each had substantially higher IC50s for all of these targets than LDN-193189 did (Table 2). Remarkably, DMH1 appeared to be very specific for ALK2 without any detectable inhibition of KDR, ALK5, AMPK, and PDGFRβ (Table 2). Importantly, the lack of ISV effects by DMH1, an exquisitely selective BMP inhibitor without any detectable KDR activity, demonstrates that the BMP signal, which is mediated by Smad1/5/8, is not required for zebrafish ISV formation.

On Western blots, DMH1, like dorsomorphin (*7*), selectively inhibited the BMP-induced Smad1/5/8 activation (Figure 4, panel c), but not the p38/MAP kinase signaling (Figure 4, panel c) or the Activin A-induced Smad2 activation (Figure 4, panel d). Consistent with the *in vitro* kinase assay result, DHM1 had no effect on VEGF-induced Flk1 phosphorylation (Figure 4, panel e). To determine whether DMH1 had subtype selectivity, we transfected the BMP signal reporter cells (*28*) with the constitutively active (ca) forms of the BMP type-I receptors ALK2, ALK3, and ALK6 (*29*) and examined DMH1's effect on BMP-responsive luciferase activity. In this assay, DMH1 effectively inhibited signaling by caALK2 and caALK3 (IC50 for both significantly less than 0.5 μM) but had negligible effect on signaling by caALK6 (Supplementary Figure S3). These results suggest that additional modifications may lead to further refinements in the subtype selectivity. From the clinical perspective, a more selective small molecule that targets just the ALK2, but not ALK3 or ALK6, would be desirable as a potential treatment for fibrodysplasia ossificans progressiva (*10, 12*).

In the above *in vivo* SAR study, DMH4 had no discernible effect on DV (Figure 5, panel b), but caused significant defects in the ISV and SIV formation (Figure 5, panel a). Additionally, 1 μM DMH4 effectively blocked angiogenesis in a Matrigel angiogenesis assay using human umbilical vein endothelial cells (Figure 5, panel c). These antiangiogenic effects of DMH4 were not mediated through BMP inhibition since, in *in vitro* BMP re-

TABLE 2. Effects of DM and five of the analogues on various *in vitro* kinase assays[a]

	IC50 (nM)				
	ALK2 (BMPR-I)	ALK5 (TGFβR-I)	AMPK	KDR (VEGFR2)	PDGFRβ
DMH1	107.9	no	no	no	no
DMH2	42.8	1578.0	3527.0	2418.0	nt
DMH3	26.7	998.0	1940.0	2062.0	nt
DMH4	3558.0	No	8038.0	161.0	nt
DM	148.1	10,760.0	234.6	25.1	nt
LDN-193189	40.7	565.0	1122.0	214.7	nt
Staurosporine	4531.0	10,640.0	<1.0	3.29	6.14

[a]Shown are the IC50s (concentrations causing 50% inhibition) of DM and the analogues for the *in vitro* kinase assays using the following purified human enzymes: the BMP type-I receptor activin receptor-like kinase 2 (ALK2/BMPR-I), the TGFβ type-I receptor activin receptor-like kinase 5 (ALK5/TGFβR-I), the VEGF type-2 receptor (VEGFR2/KDR), the AMP-activated protein kinase (AMPK), and the platelet-derived growth factor receptor-β (PDGFRβ). In *in vitro* kinase assays, DM was relatively nonspecific, targeting ALK2, AMPK, and KDR with IC50s of <250 nM. LDN-193189 was slightly more selective but still had significant effects against ALK5 and KDR. By comparison, DMH1, DMH2, and DMH3 were much more selective ALK2 inhibitors. In particular, DMH1 had no detectible activity against any of the kinases tested besides ALK2. DMH4 was a selective KDR inhibitor with modest effect on ALK2 (IC50 3.6 μM) and minimal effect on AMPK (IC50 8.0 μM). Nonspecific kinase inhibitor staurosporine was used as a control. All of the reactions were carried out in the presence of 10 μM ATP. no = no inhibition; nt = not tested.

porter and purified ALK2 kinase assays, DMH4 did not inhibit BMP signaling at such low concentrations (Figure 5, panel d; Table 2). Rather, DMH4 effectively blocked VEGF-stimulated phosphorylation of both Flk1 and the downstream mediator Akt in a dose-dependent manner (Figure 5, panels e and f). Furthermore, in an *in vitro* assay using purified human Vegfr2 (KDR), DMH4 was found to be a direct inhibitor with an IC50 of 161 nM (Table 2). Interestingly, in our *in vivo* angiogenesis analysis, the commonly utilized KDR inhibitor SU5146 (Semaxanib) (*30*), which was originally developed as an antiangiogenesis therapy, was less potent than DMH4 and not selective (Table 1).

For several compounds, the IC50s based on the *in vitro* KDR kinase assays differed dramatically from the EC50s based on their effects on ISV formation (Tables 1, 2). For example, dorsomorphin, LDN-193189, and 6LP were potent KDR inhibitors *in vitro* (IC50s of 25.1, 214.7, and 37nM, respectively), yet all were relatively poor angiogenesis inhibitors in embryos (EC50s of 5, 20, and >50 μM, respectively; Tables 1, 2). Such IC50−EC50 disparities may reflect suboptimal bioavailabilities of these compounds in later stage (~24 hpf) embryos. In summary, the zebrafish proved to be an effective platform for the rapid identification of highly selective VEGF inhibitors with excellent *in vivo* potencies and favorable physiochemical properties.

Here, we utilized zebrafish to conduct the first full-scale *in vivo* SAR study in a vertebrate model to simultaneously identify selective small molecule inhibitors of BMP and VEGF pathways, both of which are recognized as important therapeutic targets. Our analyses indicate that modification of the 3-position of the pyrazolo[1,5-*a*]pyrimidine backbone of dorsomorphin plays a critical role in determining KDR versus BMP receptor selectivity. Using this approach, we identified a potent and selective KDR inhibitor (DMH4), as well as several highly selective BMP type-I receptor inhibitors, including DMH1, which does not target any of the related signaling pathways tested. Exquisitely selective BMP inhibitors, such as DMH1, that do not affect AMPK are preferred for further development as potential therapeutic leads since they should have reduced potential for cardiotoxicity and other undesired effects compared with the compounds that inhibit AMPK. Lastly, using DMH1, we demonstrated that BMP signaling is not required for angiogenesis in early zebrafish embryos.

The *in vivo* SAR's success in identifying potent and selective inhibitors of not only BMP but also VEGF signaling demonstrates that the zebrafish provides an effective multidimensional approach to simultaneously interrogate multiple pathways on a whole organism scale. Moreover, since the *in vivo* SAR study assesses the compounds' bioactivities in live embryos, this approach is inherently likely to identify compounds having favorable physiochemical properties and excellent "drug-likeness". Thus, this approach is useful for avoiding the pitfall of pursuing "dead end" leads, such as 6LP, which have excellent *in vitro* activity yet have poor *in vivo* bioactivity. The *in vivo* SAR study contrasts with the traditional *in vitro* assay-based SAR studies that focus on identifying analogues with the highest potency. Such a "linear approach", which does not take into account selectivity and physicochemical properties until later in drug development, can lead to compounds that ultimately fail in preclinical animal models despite having a compelling biological rationale. In conclusion, we demonstrate that the zebrafish is an attractive complementary platform for pharmaceutical development that incorporates the assessment of a lead compound's *in vivo* bioactivity and selectivity earlier in the development process.

METHODS

Zebrafish Experiments. The wild-type embryos were treated with various concentrations (0.1−100 μM) of the compounds starting at 3 hpf to evaluate compounds' effects on the dorsoventral axis, and *Tg(Fli:EGFP)y1* (*18, 24*) transgenic embryos were treated from 12 hpf to evaluate the effects on ISV formation. Twenty embryos were treated per well condition. Treated embryos were manually dechorionated and observed at 24, 48, and 72 hpf.

Cells and Cell Culture. C2C12, C2C12BRA, and bovine aortic endothelial cells (BAEC) were cultured in DMEM supplemented with 10% FBS (Gibco) and 1% penicillin/ streptomycin (Cellgro). Human umbilical vein endothelial cells (HUVEC) were grown in EGM-2 Bulletkit medium (Lonza). Both BAEC and HUVEC cell lines were cultured on 0.2% gelatin-coated dishes.

Endothelial Tubule Formation. HUVEC cells (1.5×10^4) were plated on a 96-well microtiter plate precoated with 50 μL of EC-Matrix (Millipore) and were treated with DMSO or DMH4. After 15 h of incubation, tubular network formation was examined under an inverted light microscope.

Western Blotting. For VEGF signaling, confluent BAEC cells were serum-starved for 18−24 h and then treated with the compounds or DMSO for 30 min followed by 8 min of incubation with 50 ng mL^{-1} $VEGF_{165}$ (Alpha Diagnostics International, Inc.). For Smad and P38 MAPK activation, confluent HEK293 cells were

serum-starved and then treated with the compounds or DMSO for 30 min followed by 30 min incubation with BMP4 (50 ng mL^{-1}) or Activin-A (40 ng mL^{-1}). After stimulation, cells were then lysed in CelLytic-M cell lysis buffer (Sigma) supplemented with protease inhibitor cocktail (Sigma) and phosphatase inhibitor cocktail 2 (Sigma). Lysates were separated by SDS−PAGE and transferred onto PVDF membrane. The p-Flk1, p-Smad1/5/8, p-Smad2, p-AKT, p-P38MAPK, Flk1, AKT, and α-tubulin were detected by Odyssey system (Li-Cor bioscience) after incubation with the appropriate primary and secondary antibodies. Primary antibodies include antirabbit p-Flk1(Santa Cruz, 1:200 dilution), antirabbit p-Smad1/5/8 (Cell Signaling Tech, 1:1000), antirabbit p-Smad2 (Cell Signaling Tech, 1:1000), antimouse p-AKT (Cell Signaling Tech, 1:1000 dilution), antimouse p-P38MAPK (Cell Signaling Tech, 1:1000), antimouse Flk1 (Santa Cruz, 1:200 dilution), and antirabbit Akt (Cell signaling, 1:1000 dilution). The secondary antibodies include IRDye 680-conjugated goat antirabbit IgG (Li-Cor Bioscience, 1:5000 dilution) and IRDye 800CW-conjugated goat antimouse IgG (Li-Cor Bioscience, 1:5000 dilution).

BMP-Responsive Luciferase Reporter Assays. Stably transfected BMP-responsive C2C12BRA cells (containing the *Id1* promoter-firefly luciferase reporter; kind gift of D. Rifkin, NYU Medical Center (*28*)) were seeded in 96-well plates and incubated overnight with the compounds and BMP4 (50 ng mL^{-1}). The cells were then lysed, and cell extracts were then subjected to the firefly luciferase assay using Steady-Glo luciferase assay kit (Promega). The results were normalized to cell titers, as measured using Cell Titer-Glo luminescence assay (Promega). For subtype analysis, C2C12BRA cells were transiently transfected with plasmids (0.1 μg) expressing constitutively active forms of the BMP type I receptors (caALK2, caALK3 or caALK6) using Lipofectamine kit (Invitrogen) in 96 well plates; 0.1 μg of pRL-TK Renilla luciferase (Promega) was used to control for transfection efficiency. Relative activity was quantified by the ratio of firefly to Renilla luciferase activities using the dual luciferase assay kit (Promega).

Kinase Assay. All kinase assays were conducted by Reaction Biology Corp (Malvern, PA). In brief, compounds were tested at 10 concentrations by 3-fold serial dilutions starting at 30 μM, using nonspecific kinase inhibitor staurosporine as control. *In vitro* kinase reactions were carried out in the presence of 10 μM (^{33}P)γATP. Five kinases tested were the human BMP type-I receptor activin receptor-like kinase 2 (ALK-2/ACVR1), the human TGFβ type-I receptor activin receptor-like kinase 5 (Alk5/TGFβR1), the human VEGF type-II receptor (KDR/Flk-1/VEGFR2), the human AMP-activated protein kinase (AMPK/A1/B1/G1), and the human platelet-derived growth factor receptor-β (PDGFRβ).

Chemical Synthesis. The synthetic chemistry effort was concentrated on varying two aspects of the 3,6-disubstituted pyrazolo[1,5-*a*]pyrimidine core of dorsomorphin (Supplementary Figure S3): the R_1 group (C-3 of the core structure) and the R_2 group (4-phenyl group on the C-6 of the core structure). Based on the known synthetic methods available, we varied the R_1 (phenyl, 2-, 3-, and 4-pyridyl, 3-quinoline, 4-quinoline, 2-thiophene, and 2-thiazole) and R_2 (alkyl ethers). Our library synthesis was focused on common intermediates **3** and **7**, which were synthesized *via* different pathways depending on the 3-aryl substitution required (Supplementary Schemes S1, S2). For the phenyl and pyridyl derivatives, the synthesis started with the known 4-aryl-1*H*-pyrazol-5-amine **1** (*31*–*33*), which was reacted with malondialdehyde **2** to afford the pyrazolo[1,5-*a*]pyrimidine core **3** (Supplementary Scheme S1). Next, the methoxy group was deprotected, and then the phenol was alkylated under basic conditions with a number of groups affording the final products **4** (Supplementary Tables S1, S2) (*31*). For the other 3-heteroaryl-substituted pyrazolo[1,5-*a*]pyrimidine compounds **7**, the commercially available 4-bromo-1*H*-pyrazol-5-amine **5** was reacted as above with malondialdehyde **2**, which afforded the 3-bromo pyrazolo[1,5-*a*]pyrimidine core **6** (Supplementary Scheme S2). Next, **6** underwent transition-metal-catalyzed cross-coupling with either an appropriate boronic acid (*34*) or arylzinc bromide (*35*) to afford the desired **7**. Compound **7** was then reacted as above to yield the final targets **4** (Supplementary Tables S1, S2). This reaction sequence was amenable to parallel library synthesis, and utilizing this approach led to the synthesis and isolation of 63 distinct compounds. Detailed synthesis schemes are discussed in Supporting Information.

Acknowledgment: The authors thank D. Rifkin (New York University Medical Center) for the BMP-responsive reporter cell lines and T. Imamura (The JFCR Cancer Institute, Tokyo) for the constitutively active ALK constructs. The authors thank E. Catania for her critical reading of the manuscript. This work was supported by the Veterans Administration Career Development Transition Award (C.C.H.), the Developmental Grants from the Center for Research in Fibrodysplasia Ossificans Progressiva and Related Disorders (C.C.H.), the NIH K08HL081535 (C.C.H.), and the GSK Cardiovascular Research and Education Foundation (C.C.H.). J.H., C.R.H., C.W.R., and C.C.H designed the experiments and wrote the paper. J.H., J.N.H., and K.A.K. conducted zebrafish and *in vitro* analyses. J.A.L., R.N.D., and P.R.G. conducted chemical synthesis.

Supporting Information Available: This material is available free of charge *via* the Internet at http://pubs.acs.org.

Competing Interests Statement: The authors have no competing financial or personal interests to declare.

REFERENCES

1. MacCoss, M., and Baillie, T. A. (2004) Organic chemistry in drug discovery, *Science 303*, 1810–1813.
2. Zon, L. I., and Peterson, R. T. (2005) In vivo drug discovery in the zebrafish, *Nat. Rev. Drug Discovery 4*, 35–44.
3. Molina, G., Vogt, A., Bakan, A., Dai, W., Queiroz de Oliveira, P., Znosko, W., Smithgall, T. E., Bahar, I., Lazo, J. S., Day, B. W., and Tsang, M. (2009) Zebrafish chemical screening reveals an inhibitor of Dusp6 that expands cardiac cell lineages, *Nat. Chem. Biol. 5*, 680–687.
4. MacRae, C. A., and Peterson, R. T. (2003) Zebrafish-based small molecule discovery, *Chem. Biol. 10*, 901–908.
5. Hong, C. C. (2009) Large-scale small-molecule screen using zebrafish embryos, *Methods Mol. Biol. (Clifton, N.J.) 486*, 43–55.
6. Lipinski, C. A., Lombardo, F., Dominy, B. W., and Feeney, P. J. (2001) Experimental and computational approaches to estimate solubility and permeability in drug discovery and development settings, *Adv. Drug Delivery Rev. 46*, 3–26.
7. Yu, P. B., Hong, C. C., Sachidanandan, C., Babitt, J. L., Deng, D. Y., Hoyng, S. A., Lin, H. Y., Bloch, K. D., and Peterson, R. T. (2008) Dorsomorphin inhibits BMP signals required for embryogenesis and iron metabolism, *Nat. Chem. Biol. 4*, 33–41.
8. Hao, J., Daleo, M. A., Murphy, C. K., Yu, P. B., Ho, J. N., Hu, J., Peterson, R. T., Hatzopoulos, A. K., and Hong, C. C. (2008) Dorsomorphin, a selective small molecule inhibitor of BMP signaling, promotes cardiomyogenesis in embryonic stem cells, *PLoS ONE 3*, e2904.
9. Yu, P. B., Deng, D. Y., Lai, C. S., Hong, C. C., Cuny, G. D., Bouxsein, M. L., Hong, D. W., McManus, P. M., Katagiri, T., Sachidanandan, C., Kamiya, N., Fukuda, T., Mishina, Y., Peterson, R. T., and Bloch, K. D. (2008) BMP type I receptor inhibition reduces heterotopic [corrected] ossification, *Nat. Med. 14*, 1363–1369.

10. Shen, Q., Little, S. C., Xu, M., Haupt, J., Ast, C., Katagiri, T., Mundlos, S., Seemann, P., Kaplan, F. S., Mullins, M. C., and Shore, E. M. (2009) The fibrodysplasia ossificans progressiva R206H ACVR1 mutation activates BMP-independent chondrogenesis and zebrafish embryo ventralization, *J. Clin. Invest. 119*, 3462–3472.
11. Kaplan, F. S., Xu, M., Seemann, P., Connor, J. M., Glaser, D. L., Carroll, L., Delai, P., Fastnacht-Urban, E., Forman, S. J., Gillessen-Kaesbach, G., Hoover-Fong, J., Koster, B., Pauli, R. M., Reardon, W., Zaidi, S. A., Zasloff, M., Morhart, R., Mundlos, S., Groppe, J., and Shore, E. M. (2009) Classic and atypical fibrodysplasia ossificans progressiva (FOP) phenotypes are caused by mutations in the bone morphogenetic protein (BMP) type I receptor ACVR1, *Hum. Mutat. 30*, 379–390.
12. Shore, E. M., Xu, M., Feldman, G. J., Fenstermacher, D. A., Cho, T. J., Choi, I. H., Connor, J. M., Delai, P., Glaser, D. L., LeMerrer, M., Morhart, R., Rogers, J. G., Smith, R., Triffitt, J. T., Urtizberea, J. A., Zasloff, M., Brown, M. A., and Kaplan, F. S. (2006) A recurrent mutation in the BMP type I receptor ACVR1 causes inherited and sporadic fibrodysplasia ossificans progressiva, *Nat. Genet. 38*, 525–527.
13. Zhou, G., Myers, R., Li, Y., Chen, Y., Shen, X., Fenyk-Melody, J., Wu, M., Ventre, J., Doebber, T., Fujii, N., Musi, N., Hirshman, M. F., Goodyear, L. J., and Moller, D. E. (2001) Role of AMP-activated protein kinase in mechanism of metformin action, *J. Clin. Invest. 108*, 1167–1174.
14. Russell, R. R., 3rd, Li, J., Coven, D. L., Pypaert, M., Zechner, C., Palmeri, M., Giordano, F. J., Mu, J., Birnbaum, M. J., and Young, L. H. (2004) AMP-activated protein kinase mediates ischemic glucose uptake and prevents postischemic cardiac dysfunction, apoptosis, and injury, *J. Clin. Invest. 114*, 495–503.
15. Sasaki, H., Asanuma, H., Fujita, M., Takahama, H., Wakeno, M., Ito, S., Ogai, A., Asakura, M., Kim, J., Minamino, T., Takashima, S., Sanada, S., Sugimachi, M., Komamura, K., Mochizuki, N., and Kitakaze, M. (2009) Metformin prevents progression of heart failure in dogs: role of AMP-activated protein kinase, *Circulation 119*, 2568–2577.
16. Vazquez-Martin, A., Oliveras-Ferraros, C., Lopez-Bonet, E., and Menendez, J. A. (2009) AMPK: Evidence for an energy-sensing cytokinetic tumor suppressor, *Cell Cycle 8*, 3679–3683.
17. Bussmann, J., Lawson, N., Zon, L., and Schulte-Merker, S. (2008) Zebrafish VEGF receptors: a guideline to nomenclature, *PLoS Genet. 4*, e1000064.
18. Isogai, S., Lawson, N. D., Torrealday, S., Horiguchi, M., and Weinstein, B. M. (2003) Angiogenic network formation in the developing vertebrate trunk, *Development (Cambridge, U.K.) 130*, 5281–5290.
19. Covassin, L. D., Villefranc, J. A., Kacergis, M. C., Weinstein, B. M., and Lawson, N. D. (2006) Distinct genetic interactions between multiple Vegf receptors are required for development of different blood vessel types in zebrafish, *Proc. Natl. Acad. Sci. U.S.A. 103*, 6554–6559.
20. Habeck, H., Odenthal, J., Walderich, B., Maischein, H., and Schulte-Merker, S. (2002) Analysis of a zebrafish VEGF receptor mutant reveals specific disruption of angiogenesis, *Curr. Biol. 12*, 1405–1412.
21. Heinke, J., Wehofsits, L., Zhou, Q., Zoeller, C., Baar, K. M., Helbing, T., Laib, A., Augustin, H., Bode, C., Patterson, C., and Moser, M. (2008) BMPER is an endothelial cell regulator and controls bone morphogenetic protein-4-dependent angiogenesis, *Circ. Res. 103*, 804–812.
22. Scharpfenecker, M., van Dinther, M., Liu, Z., van Bezooijen, R. L., Zhao, Q., Pukac, L., Lowik, C. W., and ten Dijke, P. (2007) BMP-9 signals via ALK1 and inhibits bFGF-induced endothelial cell proliferation and VEGF-stimulated angiogenesis, *J. Cell Sci. 120*, 964–972.
23. Fraley, M. E., Rubino, R. S., Hoffman, W. F., Hambaugh, S. R., Arrington, K. L., Hungate, R. W., Bilodeau, M. T., Tebben, A. J., Rutledge, R. Z., Kendall, R. L., McFall, R. C., Huckle, W. R., Coll, K. E., and Thomas, K. A. (2002) Optimization of a pyrazolo[1,5-*a*]pyrimidine class of KDR kinase inhibitors: improvements in physical properties enhance cellular activity and pharmacokinetics, *Bioorg. Med. Chem. Lett. 12*, 3537–3541.
24. Lawson, N. D., and Weinstein, B. M. (2002) In vivo imaging of embryonic vascular development using transgenic zebrafish, *Dev. Biol. 248*, 307–318.
25. Daniels, R. N., Kim, K., Lebois, E. P., Muchalski, H., Hughes, M., and Lindsley, C. W. (2008) Microwave-assisted protocols for the expedited synthesis of pyrazolo[1,5-*a*] and [3,4-*d*]pyrimidines, *Tetrahedron Lett. 49*, 305–310.
26. Fraley, M. E., Hoffman, W. F., Rubino, R. S., Hungate, R. W., Tebben, A. J., Rutledge, R. Z., McFall, R. C., Huckle, W. R., Kendall, R. L., Coll, K. E., and Thomas, K. A. (2002) Synthesis and initial SAR studies of 3,6-disubstituted pyrazolo[1,5-*a*]pyrimidines: a new class of KDR kinase inhibitors, *Bioorg. Med. Chem. Lett. 12*, 2767–2770.
27. Cuny, G. D., Yu, P. B., Laha, J. K., Xing, X., Liu, J. F., Lai, C. S., Deng, D. Y., Sachidanandan, C., Bloch, K. D., and Peterson, R. T. (2008) Structure-activity relationship study of bone morphogenetic protein (BMP) signaling inhibitors, *Bioorg. Med. Chem. Lett. 18*, 4388–4392.
28. Zilberberg, L., ten Dijke, P., Sakai, L. Y., and Rifkin, D. B. (2007) A rapid and sensitive bioassay to measure bone morphogenetic protein activity, *BMC Cell Biol. 8*, 41.
29. Fujii, M., Takeda, K., Imamura, T., Aoki, H., Sampath, T. K., Enomoto, S., Kawabata, M., Kato, M., Ichijo, H., and Miyazono, K. (1999) Roles of bone morphogenetic protein type I receptors and Smad proteins in osteoblast and chondroblast differentiation, *Mol. Biol. Cell 10*, 3801–3813.
30. Fong, T. A., Shawver, L. K., Sun, L., Tang, C., App, H., Powell, T. J., Kim, Y. H., Schreck, R., Wang, X., Risau, W., Ullrich, A., Hirth, K. P., and McMahon, G. (1999) SU5416 is a potent and selective inhibitor of the vascular endothelial growth factor receptor (Flk-1/KDR) that inhibits tyrosine kinase catalysis, tumor vascularization, and growth of multiple tumor types, *Cancer Res. 59*, 99–106.
31. Daniels, R. N., Kim, K., Lebois, E. P., Muchalski, H., Hughes, M., and Lindsley, C. W. (2008) Microwave-assisted protocols for the expedited synthesis of pyrazolo[1,5-*a*] and [3,4-*d*]pyrimidines, *Tetrahedron Lett. 49*, 305–310.
32. Fraley, M. E., Hoffman, W. F., Rubino, R. S., Hungate, R. W., Tebben, A. J., Rutledge, R. Z., McFall, R. C., Huckle, W. R., Kendall, R. L., Coll, K. E., and Thomas, K. A. (2002) Synthesis and initial SAR studies of 3,6-disubstituted pyrazolo[1,5-*a*]pyrimidines: a new class of KDR kinase inhibitors, *Bioorg. Med. Chem. Lett. 12*, 2767–2770.
33. Fraley, M. E., Rubino, R. S., Hoffman, W. F., Hambaugh, S. R., Arrington, K. L., Hungate, R. W., Bilodeau, M. T., Tebben, A. J., Rutledge, R. Z., Kendall, R. L., McFall, R. C., Huckle, W. R., Coll, K. E., and Thomas, K. A. (2002) Optimization of a pyrazolo[1,5-*a*]pyrimidine class of KDR kinase inhibitors: improvements in physical properties enhance cellular activity and pharmacokinetics, *Bioorg. Med. Chem. Lett. 12*, 3537–3541.
34. Miyaura, N., and Suzuki, A. (1995) Palladium-catalyzed cross-coupling reactions of organoboron compounds, *Chem. Rev. 95*, 2457–2483.
35. King, A. O., Okakadao, N., and E.-i, N. (1977) Highly general stereo-, regio-, and chemo-selective synthesis of terminal and internal conjugated enynes by the Pd-catalyzed reaction of alkynylzinc reagents with alkenyl halides, *J. Chem. Soc., Chem. Comm.* 683–684.